Supplementary Information

Summer fluxes of methane and carbon dioxide from a pond and floating mat in a continental Canadian peatland

M. Burger[1,2], S. Berger[1,2], I. Spangenberg[1,2] and C. Blodau[1,2]

[1] Ecohydrology and Biogeochemistry Group, Institute of Landscape Ecology, University of Münster, Germany

[2] School of Environmental Sciences, University of Guelph, Canada

Correspondence to: C. Blodau (christian.blodau@uni-muenster.de)

1. Chamber flux measurements

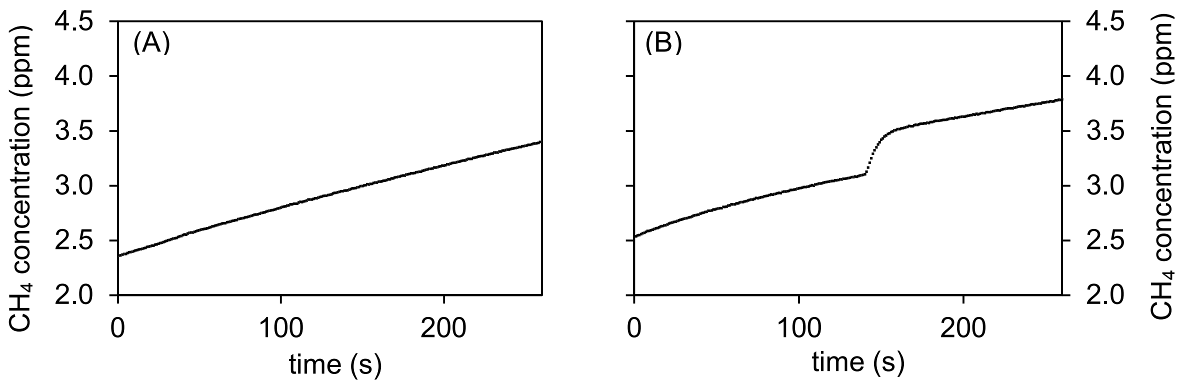

Figure S1. Example of a concentration time series with a constant slope representing diffusive CH_4 flux or continuous flux of micro-bubbles (panel A) and example of a concentration time series including a CH_4 bubble event visible by a sudden increase of slope over a short duration (panel B).

2. CO_2 flux calculation with the gradient method

CO_2 fluxes across the air-water interface were estimated according to the boundary layer equation approach, equation (1).

$$F = k_{CO_2} \cdot (c_{water} - c_{atm}) \quad (1)$$

F	CO_2 flux (mmol m^{-2} h^{-1})
k_{CO_2}	gas transfer velocity (m h^{-1})
c_{water}	CO_2 concentration in the surface water (mmol m^{-3})
c_{atm}	theoretical CO_2 concentration of the surface water in equilibrium with the atmospheric CO_2 concentration (mmol m^{-3})

c_{water} and c_{atm} were calculated with Henry's law from the CO_2 mixing ratios measured in the surface water and the atmosphere using Henry's law constants (Sander, 1999) corrected for surface water temperature. The gas transfer velocity k_{CO_2} was calculated from the gas transfer velocity normalized to a Schmidt number of 600 (k_{600}) according to equation (2) (Crusius and Wanninkhof, 2003).

$$k_{CO_2} = k_{600} \cdot \left(\frac{Sc_{CO_2}}{600}\right)^{-b} \quad (2)$$

k_{CO_2}	gas transfer velocity (m h^{-1})
k_{600}	gas transfer velocity normalized to a Schmidt number of 600 (m h^{-1})
Sc_{CO_2}	Schmidt number for CO_2 corrected for temperature (−)
600	Schmidt number of CO_2 at 20 °C
B	$\frac{1}{2}$ for wind speed > 3 m s^{-1} $\frac{2}{3}$ for wind speed ≤ 3 m s^{-1}

k_{600} depends on the wind speed at a height of 10 m according to the empirical relationship defined by Cole and Caraco (1998) (equation 3). Sc_{CO_2} was calculated as a function of water temperature (equation 5; Wanninkhof, 1992).

$$k_{600} = 0.0207 + 0.00215 \cdot {U_{10}}^{1.7} \quad (3)$$

k_{600}	gas transfer velocity normalized to a Schmidt number of 600 (m h^{-1})
U_{10}	wind speed at 10 m height (m s^{-1})

$$Sc_{CO_2} = 1911.1 - 118.11 \cdot T + 3.4527 \cdot T^2 - 0.04132 \cdot T^3 \quad (4)$$

Sc_{CO_2}	Schmidt number for CO_2 corrected for temperature (−)
T	water temperature (°C)

Wind speed at a height of 10 m was estimated from the wind speed measurements at the weather station at a height of 2.5 m according to equation (5) (Singh et al., 2007).

$$U_2 = U_1 \cdot \left(\frac{h_2}{h_1}\right)^{\frac{1}{6}} \quad (5)$$

U_2	estimated wind speed (m s^{-1}) at h_2
U_1	measured wind speed (m s^{-1}) at h_1
h_2	height (m) of the estimated wind speed U_2; 10 m
h_1	height (m) of the measured wind speed U_1; 2.5 m

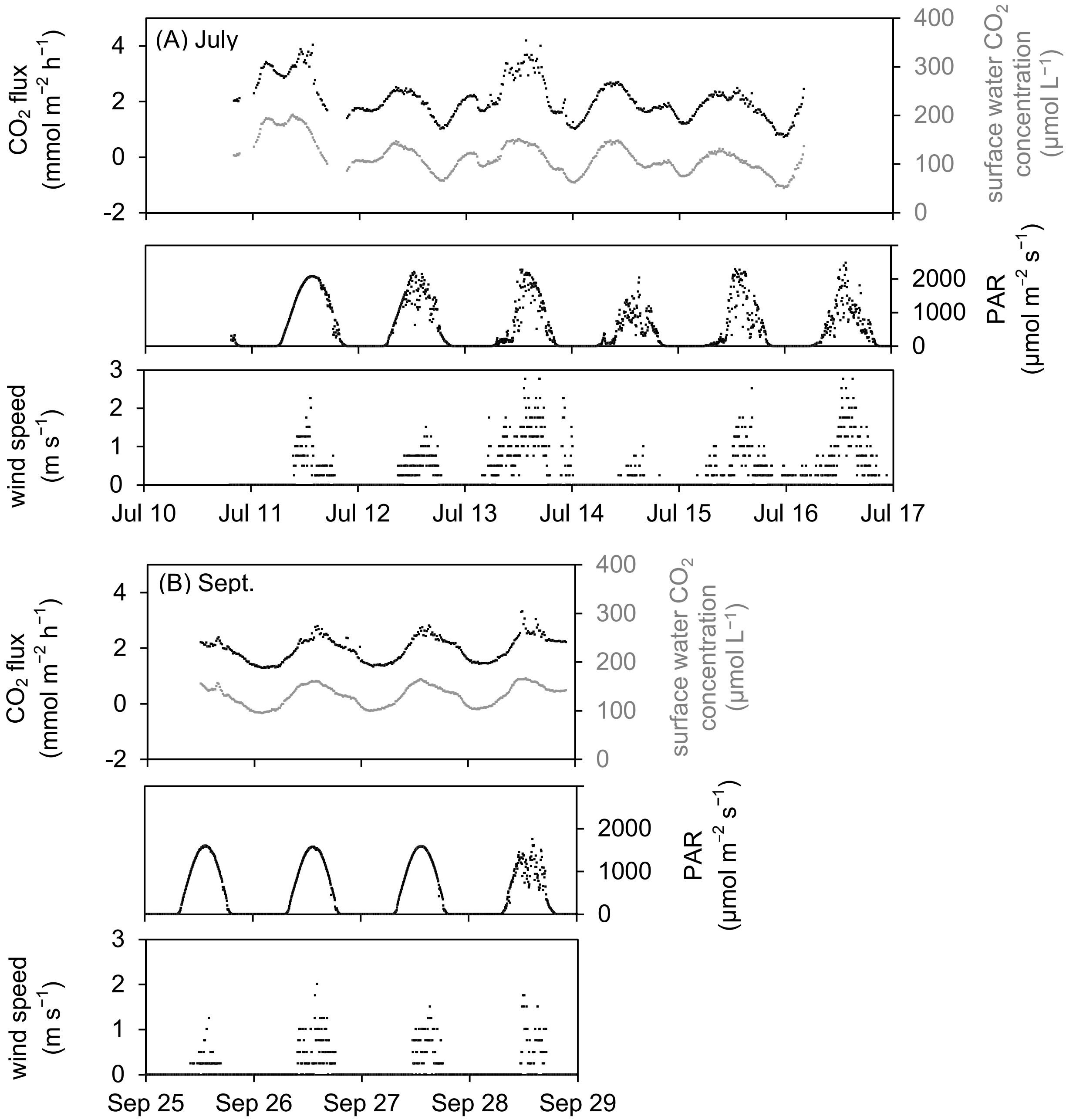

Figure S2: CO_2 concentrations in the surface water of the pond (gray symbols), CO_2 fluxes calculated with the gradient method (black symbols), photosynthetically active radiation and wind speed (both 5 min averages) during two periods in July (panel A) and September (panel B) 2014.

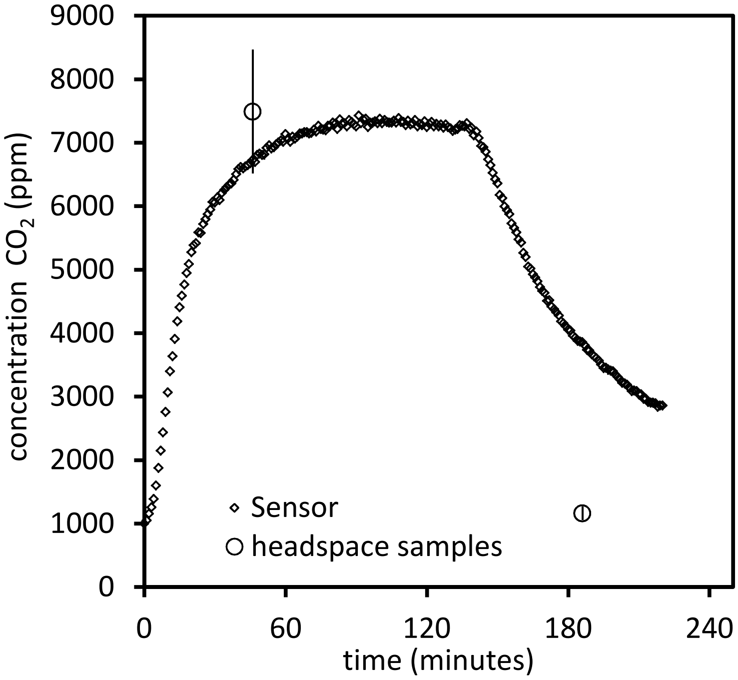

Figure S3: To estimate the response time of silicone-covered NDI CO_2 sensors, about 10 L of water were filled in a bucket and acidified to pH 4 by adding 1 M HCl. Subsequently CO_2 and air were bubbled through the solution from a gas cylinder and using an air pump, respectively, to adjust dissolved CO_2 concentrations and mix the water. Headspace samples (5 mL water, 7.5 mL gas phase) were taken and analyzed by gas chromatography as described in the Methods section. After 124 minutes CO_2 supply was stopped but air continuously pumped for another hour. The results suggest that equilibration was > 90% after one hour with increasing concentration and somewhat more delayed with decreasing concentrations.

Figure S4: Studied pond with algal mat in the beginning of August 2014 (above) and without algal mat in the end of September 2014 (below).

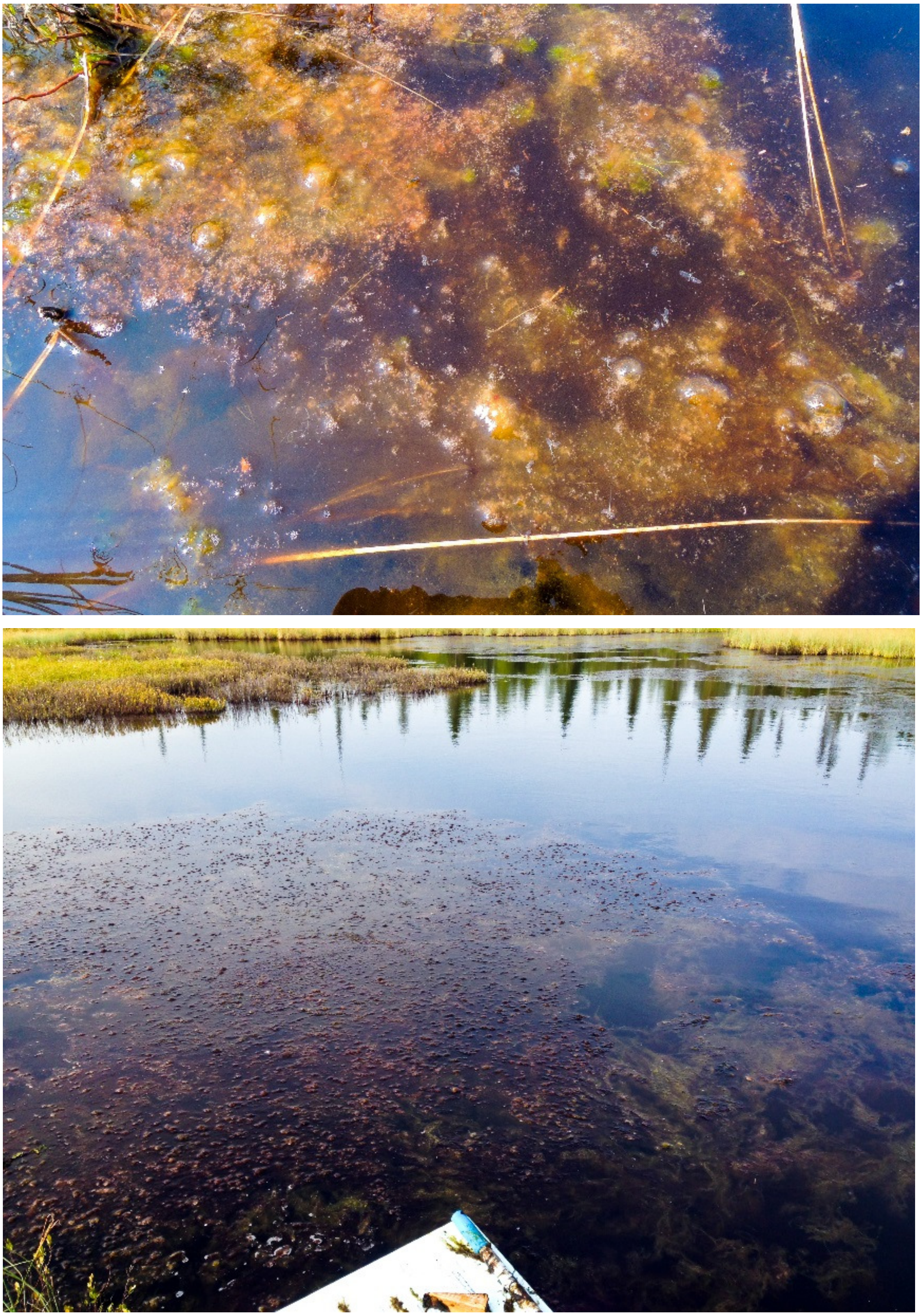

Figure S5: Close-up of algal mat in the beginning of August 2014 (above).

Table S1. Plant species composition of the floating mat, the surrounding treed area and the chamber measurement plots m1 to m3 (section **Error! Reference source not found.**); c: common, s: scattered, r: rare, –: absent; species nomenclature according to Hellquist and Crow (1999a), (1999b), Newmaster and Ragupathy (2012).

species	abundance				
			plot		
	floating mat	treed area	m1	m2	m3
Sphagnum angustifolium (Russ.) C. Jens.	c	C	c	c	c
Sphagnum magellanicum Brid.	c	C	–	–	–
Sphagnum fuscum (Schimp.) Klinggr.	–	S	–	–	–
Sphagnum wulfianum Girg.	–	S	–	–	–
Larix laricina (DuRoi) K. Koch	–	c-s	–	–	–
Picea mariana (Mill.) BSP.	–	c-s	–	–	–
Pinus strobus L.	–	R	–	–	–
Eleocharis smallii Britt.	–	S	–	–	–
Eriophorum vaginatum L.	s	S	–	–	–
Eriophorum virginicum L.	s	S	–	–	–
Dulichium arundinaceum (L.) Britt.	r	–	–	–	–
Rhynchospora alba (L.) Vahl	c	–	s	c-s	s
Carex aquatilis Wahlenb.	s	–	r	–	s
Carex oligosperma Michx.	s	–	–	–	–
Carex magellanica Lam.	s	–	–	–	–
Carex disperma Dew.	–	S	–	–	–
Myrica gale L.	r	s-r	–	–	–
Betula pumila L.	–	S	–	–	–
Sarracenia purpurea L.	s	–	–	r	–
Drosera rotundifolia L.	r	–	–	–	–
Populus sp.	–	S	–	–	–
Rhododendron groenlandicum (Oeder) Kron & Judd	r	C	–	–	–
Kalmia polifolia Wang.	s	S	–	r	–
Kalmia angustifolia L.	–	R	–	–	–
Andromeda glaucophylla Link	s	S	–	r	–
Vaccinium oxycoccos L.	s	S	–	–	r
Vaccinium myrtilloides Hook.	–	S	–	–	–
Vaccinium macrocarpon Ait.	–	S	–	–	–
Vaccinium corymbosum L.	–	S	–	–	–
Vaccinium uliginosum L.	–	R	–	–	–
Chamaedaphne calyculata (L.) Moench	s	c-s	s	s	s
Aronia melanocarpa (Michx.) Ell.	–	S	–	–	–
Cypripedium parviflorum Salisb.	–	R	–	–	–
Cypripedium reginae Walt.	–	R	–	–	–

Table S2. Environmental variables measured at the study site with the corresponding instruments, measuring height, orientation, temporal resolution and accuracy.

Variable	instrument	measuring height or depth[a]	orientation	temporal resolution	accuracy
air temperature (°C)	Temperature/RH Smart Sensor, S-THB-M002, Onset	+ 2.0 m	north	5 min	± 0.21 °C
relative humidity (%)	Temperature/RH Smart Sensor, S-THB-M002, Onset	+ 2.0 m	north	5 min	± 2.5 %
wind speed (m s^{-1})	Wind Speed Smart Sensor, S-WSA-M002, Onset	+ 2.5 m	west-southwest	5 min	± 1.1 m s^{-1} or 4 % (whichever is greater)
wind direction (°)	Wind Direction Smart Sensor, S-WDA-M002, Onset	+ 2.5 m	east-northeast	5 min	± 5°
photosynthetically active radiation (µmol m^{-2} s^{-1})	Photosynthetic Light (PAR) Smart Sensor, S-LIA-M002, Onset	+ 2.3 m	south	5 min	± 5 µmol m^{-2} s^{-1} or 5 % (whichever is greater)
precipitation (mm)	.2mm Rainfall Smart Sensor, S-RGB-M002, Onset	+ 1.0 m	west-northwest	5 min	± 1 %
water temperature pond (°C)	CTD-Diver, Schlumberger	− 0.2 m	–	5 min	± 0.1 °C
temperature floating mat (°C)	Air/Water/Soil Temp Sensor, TMC6-HD, Onset	− 5 and − 10 cm	–	5 min	± 0.25 °C
air pressure (kPa)	Enclosed Path CO_2/ H_2O Analyzer, LI-7200, LI-COR	+ 5.0 m	–	30 min	± 4 %

[a]: indicated by positive (height) or negative sign (depth)

Table S3. Distance from the floating mat and water depth of the chamber measurement plots of the pond.

plot	distance from the floating mat (m)	water depth (m)
p1	4.55	0.73
p2	3.76	0.83
p3	3.15	0.77
p4	1.91	0.62
p5	0.80	0.52
p6	0.73	0.42

Table S4. CH_4 fluxes from the studied peatland, floating mat and pond in comparison to CH_4 fluxes reported from northern peatlands, floating mats and ponds in literature.

System	Location	CH_4 fluxes (mmol m^{-2} h^{-1}) minimum	median	mean	maximum	time horizon	reference
Peatlands							
peatland site, Wylde Lake Bog	Ontario, Canada	0.00	0.32	0.71	28.13	July to Sept.	this study
Bog	Ontario, Canada			0.07		July and Aug.	Dinsmore et al. (2009)
Fen	Michigan, USA			0.02		April to Oct.	Ballantyne et al. (2014)
fen hummock fen lawns and hollows	Quebec, Canada			0.07 0.09		two years	Trudeau et al. (2013)
2 fens, 1 bog	Ontario, Canada			0.04		June to Oct.	Hamilton et al. (1994)
poor fen	Quebec, Canada	0.00	0.11		0.38	May to Sept.	Strack et al. (2006)
bog hummocks bog lawns and ponds	Ontario, Canada			0.01 0.26		May to Oct.	Moore et al. (2011)
floating mats							
floating mat in Wylde Lake Bog	Ontario, Canada	0.06	0.64	1.52	14.98	July to Sept.	this study
floating mat on thermokarst pond in bog	Siberia, Russia			0.14		one year	Flessa et al. (2008)
floating mats in bog *Sphagnum* *Phragmites australis* *Menyanthes trifoliata*	central Japan			 0.18 0.76 1.17		April to Oct.	Sugimoto and Fujita (1997)
Ponds							
pond in Wylde Lake Bog area: 847 m^2 depth: 0.5 m	Ontario, Canada	0.00	0.14	0.22	2.00	July to Sept.	this study
Beaver pond depth: 0.8 m	Ontario, Canada			0.01		July and Aug.	Dinsmore et al. (2009)
2 fen pools area: 65 and 200 m^2 depth: 0.4 and 0.9 m	Quebec, Canada			0.50 and 0.23		2 years	Trudeau et al. (2013)
24 bog and fen ponds area: 32 to 41620 m^2 depth: 0.1 to 2.0 m	Ontario, Canada			0.38		June to Oct.	Hamilton et al. (1994)
fen pond area: 10000 m^2 max. depth: 3.2 m	northern Finland			0.48		May to Sept.	Huttunen et al. (2002)
5 bog pools area: 128 to 2563 m^2 depth: 0.4 to 2.0 m	Quebec, Canada	0.00 to 0.01		0.01 to 0.20	0.04 to 0.41	1.5 years	Pelletier et al. (2014)
fen pond area: 5000 m^2 depth: 1 m	Siberia, Russia	0.03	0.06	0.11	0.31	July to Sept.	Repo et al. (2007)

Table S5. Daytime maximum net ecosystem exchange (NEE) and ecosystem respiration (ER) of the studied peatland and floating mat in comparison to respective values from temperate peatlands reported in literature.

System	Location	maximum NEE and ER (mmol m^{-2} h^{-1})				time horizon	reference
		minimum	median	mean	maximum		
peatland site, Wylde Lake Bog	Ontario, Canada	−36.96 2.61	−16.98 11.98	−18.73 13.59	−8.10 36.93	July to Sept.	this study
floating mat in Wylde Lake Bog	Ontario , Canada	−11.46 0.53	−4.81 6.77	−4.40 6.41	0.71 13.45	July to Sept.	this study
Bog	Ontario, Canada			−29.7 15.3		May to Sept.	Larmola et al. (2013)
Fen	Michigan, USA			−7.56 8.64		April to Oct.	Ballantyne et al. (2014)

Table S6. CO_2 fluxes from the studied pond in comparison to CO_2 fluxes from ponds in northern peatlands reported in literature.

System	location	CO_2 fluxes (mmol m^{-2} h^{-1})				time horizon	reference
		minimum	median	mean	maximum		
pond in Wylde Lake Bog area: 847 m^2 depth: 0.5 m	Ontario, Canada	−0.75	1.16	1.32	4.59	July to Sept.	this study
Beaver pond depth: 0.8 m	Ontario, Canada			13.48		July and Aug.	Dinsmore et al. (2009)
24 bog and fen ponds area: 32 to 41620 m^2 depth: 0.1 to 2.0 m	Ontario, Canada			6.96		June to Oct.	Hamilton et al. (1994)
peatland pond area: 10000 m^2 max. depth: 3.2 m	northern Finland			0.50		May to Sept.	Huttunen et al. (2002)
5 bog pools area: 128 to 2563 m^2 depth: 0.4 to 2.0 m	Quebec, Canada	0.04 to 0.34		0.32 to 0.80	0.53 to 1.98	1.5 years	Pelletier et al. (2014)
fen pond area: 5000 m^2 depth: 1 m	Siberia, Russia	0.85	1.42	1.52	2.94	July to Sept.	Repo et al. (2007)

References

Ballantyne, D.M., Hribljan, J.A., Pypker, T.G., Chimner, R.A.: Long-term water table manipulations alter peatland gaseous carbon fluxes in Northern Michigan. Wetlands Ecology and Management 22, 35–47, 2014.

Cole, J.J., Caraco, N.F.: Atmospheric exchange of carbon dioxide in a low-wind oligotrophic lake measured by the addition of SF_6. Limnology and Oceanography 43, 647–656, 1998.

Crusius, J., Wanninkhof, R.: Gas transfer velocities measured at low wind speed over a lake. Limnology and Oceanography 48, 1010–1017, 2003.

Dinsmore, K.J., Billett, M.F., Moore, T.R.: Transfer of carbon dioxide and methane through the soil-water-atmosphere system at Mer Bleue peatland, Canada. Hydrological Processes 23, 330–341, 2009.

Flessa, H., Rodionov, A., Guggenberger, G., Fuchs, H., Magdon, P., Shibistova, O., Zrazhevskaya, G., Mikheyeva, N., Kasansky, O., Blodau, C.: Landscape controls of CH_4 fluxes in a catchment of the forest tundra ecotone in northern Siberia. Global Change Biology 14, 2040–2056, 2008.

Hamilton, J.D., Kelly, C.A., Rudd, J.W.M., Hesslein, R.H., Roulet, N.T.: Flux to the atmosphere of CH_4 and CO_2 from wetland ponds on the Hudson Bay lowlands (HBLs). Journal of Geophysical Research 99, 1495–1510, 1994.

Hellquist, C.B., Crow, G.E.: Aquatic and Wetland Plants of Northeastern North America, A Revised and Enlarged Edition of Norman C. Fassett’s A Manual of Aquatic Plants, Volume II Angiosperms Monocotyledons. Madison, 1999a.

Hellquist, C.B., Crow, G.E.: Aquatic and Wetland Plants of Northeastern North America, A Revised and Enlarged Edition of Norman C. Fassett’s A Manual of Aquatic Plants, Volume I Pteridophytes, Gymnosperms, and Angiosperms Dicotyledons. Madison, 1999b.

Huttunen, J.T., Väisänen, T.S., Heikkinen, M., Hellsten, S., Nykänen, H., Nenonen, O., Martikainen, P.J.: Exchange of CO_2, CH_4 and N_2O between the atmosphere and two northern boreal ponds with catchments dominated by peatlands or forests. Plant and Soil 242, 137–146, 2002.

Larmola, T., Bubier, J.L., Kobyljanec, C., Basiliko, N., Juutinen, S., Humphreys, E.R., Preston, M., Moore, T.R.: Vegetation feedbacks of nutrient addition lead to a weaker carbon sink in an ombrotrophic bog. Global Change Biology 19, 3729–3739, 2013.

Moore, T.R., De Young, A., Bubier, J.L., Humphreys, E.R., Lafleur, P.M., Roulet, N.T.: A Multi-Year Record of Methane Flux at the Mer Bleue Bog, Southern Canada. Ecosystems 14, 646–657, 2011.

Newmaster, S.G., Ragupathy, S.: Flora Ontario – Integrated Botanical Information System (FOIBIS). University of Guelph. URL http://www.uoguelph.ca/foibis/ (accessed April 24th, 2015), 2012.

Pelletier, L., Strachan, I.B., Garneau, M., Roulet, N.T.: Carbon release from boreal peatland open water pools: Implication for the contemporary C exchange. Journal of Geophysical Research: Biogeosciences 119, 207–222, 2014.

Repo, M.E., Huttunen, J.T., Naumov, A. V., Chichulin, A. V., Lapshina, E.D., Bleuten, W., Martikainen, P.J.: Release of CO_2 and CH_4 from small wetland lakes in western Siberia. Tellus 59B, 788–796, 2007.

Sander, R.: Compilation of Henry's Law Constants for Inorganic and Organic Species of Potential Importance in Environmental Chemistry. Max-Planck Institute of Chemistry, Mainz, 1999.

Singh, S., Bhatti, T.S., Kothari, D.P.: Wind Power Estimation Using Artificial Neural Network. Journal of Energy Engineering 133, 46–52, 2007.

Strack, M., Waller, M.F., Waddington, J.M.: Sedge succession and peatland methane dynamics: A potential feedback to climate change. Ecosystems 9, 278–287, 2006.

Sugimoto, A., Fujita, N.: Characteristics of methane emissions from different vegetations on a wetland. Tellus 49B, 382–392, 1997.

Trudeau, N.C., Garneau, M., Pelletier, L.: Methane fluxes from a patterned fen of the northeastern part of the La Grande river watershed, James Bay, Canada. Biogeochemistry 113, 409–422, 2013.

Wanninkhof, R.: Relationship Between Wind Speed and Gas Exchange Over the Ocean. Journal of Geophysical Research 97, 7373–7382, 1992.